Key Engineering Materials
ISSN: 1662-9795, Vol. 926, pp 416-425
doi:10.4028/p-qfc820

Submitted: 2021-12-08
Revised: 2022-01-28
Accepted: 2022-01-28
Online: 2022-07-22

Modeling Friction in HyperXtrude for Hot Forward Extrusion Simulation of EN AW 6060 and EN AW 6082 Alloys

Sheikh Enamul Hoque[a*], Sindre Hovden[b], Stefan Culic[c], Jürgen A. Nietsch[d], Johannes Kronsteiner[e] and Dieter Horwatitsch[f]

LKR Light Metals Technologies Ranshofen, AIT Austrian Institute of Technology
Lamprechtshausener Str. 61, 5282 Ranshofen, Austria

[a]sheikh.hoque@ait.ac.at, [b]sindre.hovden@ait.ac.at, [c]stefan.culic@ait.ac.at,
[d]juergen.nietsch@ait.ac.at, [e]Johannes.kronsteiner@ait.ac.at, [f]dieter.horwatitsch@ait.ac.at

Keywords: Aluminum extrusion, Friction modeling, HyperXtrude.

Abstract. In this work, different friction models available in HyperXtrude had been investigated in the context of hot forward extrusion simulation of aluminum alloys. Extrusion trials were carried out for EN AW 6060 and EN AW 6082 at different temperatures and ram speeds. The extrusion forces as well as material temperatures near the exit of the die were recorded and used for the validation of the simulations. FE-simulations of each extrusion trial were carried out in HyperXtrude. Initially, friction models were calibrated for only two extrusion trials. Then, these calibrated friction models were used to simulate the extrusion trials with different process parameters. Reasonably good agreements were observed between experiments and simulations in terms of extrusion forces. However, the simulations overpredicted the material temperature by almost up to 40 °C for extrusion trials with high ram speed.

Introduction

Extrusion processes are highly sensitive to frictional effects [1, 2]. Hence, accurate friction modeling is necessary for a realistic extrusion process simulation. Two most common friction models used in metal forming simulations are: Coulomb friction model and Tresca (shear) friction model [3]. Coulomb model correlates critical sliding shear stress to normal compressive stress by a friction coefficient and is appropriate for low contact pressure. At high contact pressure, Tresca model is more appropriate which correlates critical sliding shear stress with shear flow stress of the softer contact body. A third friction model which combines Coulomb and Tresca is Wanheim and Bay's friction model [4]. Many other friction models exist in the literatures [5-9]. However, not all of them are available in commercial codes.

HyperXtrude is one of the most used commercial solvers for extrusion process simulation. It uses Arbitrary Lagrangian–Eulerian (ALE) technique combining advantages of both Lagrangian and Eulerian methods. Since the mesh and the material are detached in ALE, the inevitable mesh distortion and regeneration associated with large deformation, as seen in Lagrangian codes, is avoided. There are five different friction models in HyperXtrude: Coulomb, Slip, Stick, Viscoplastic, and Slip Velocity. Slip friction allows material particles to completely slip over the boundary surface while Stick friction implies that the moving material particles adhere to the boundary surface. These are the two-extreme situations of Viscoplastic friction model in which the frictional shear stress is a function of the flow stress as well as the pressure. Slip Velocity model describes the frictional shear stress as a linear function of the slip velocity.

In common practice, a full sticking condition around the billet surface and a visco-plastic condition at the bearing interface is applied in extrusion simulation [10-14]. A comparative study on different friction models from different solvers can be found in [15]. However, it is focused on Coulomb and Tresca model. Thus, a thorough study on different friction models, especially their transferability to different processing conditions (temperature, ram speed) is still missing. Hence, in this work, all five friction models available in HyperXtrude had been studied in terms of their accuracy, rate of convergence as well as validity for different process conditions.

Experimental Work

The extrusion experiments were conducted on a Müller NEHP 1500.01 semi-industrial scale extrusion press with a maximum force of 1.5 MN and a 50 mm inner diameter container. The benchmark tool (Fig. 1, left) used in this work produces a round bar extrudate with 10 mm diameter (Fig. 1, right). Thus, the extrusion ratio $ER = A_{container} / A_{extrudate} = 25$. Typical ER value for hard alloys can go up to 40 [16], while soft alloys can be extruded at even higher extrusion ratios. The cylindrical billets (Fig. 1, right) had a dimeter of 48.5 mm and height of 180 mm.

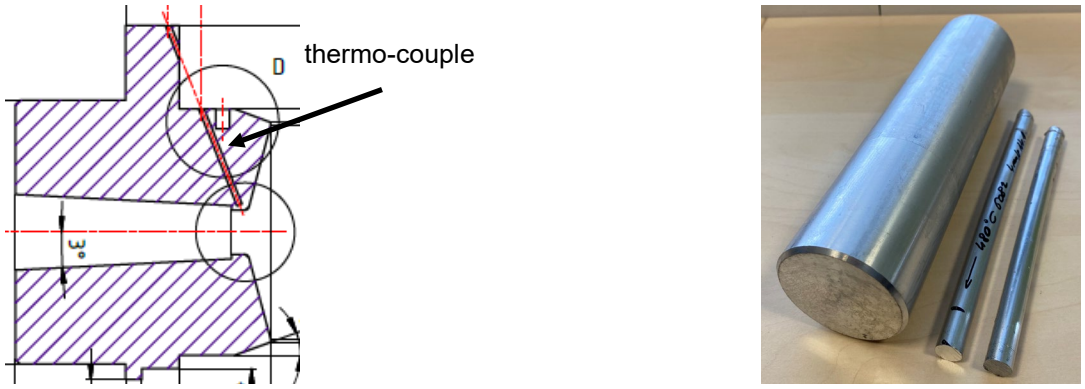

Fig. 1: (left) benchmark tool, (right) billet and extrudate.

Two aluminum alloys (EN AW 6060 and EN AW 6082) were used in the experimental study. Each alloy was extruded at two temperatures (460 °C and 480 °C). For each temperature, extrusion trials were carried out at three ram speeds (1 mm/s, 4 mm/s, 8 mm/s). Each test was repeated twice. The full factorial plan is presented in Table 1.

Table 1: DOE of extrusion trials.

Trials	Alloy	Temperature of the Billet, Container and Die [°C]	Ram Speed [mm/s]	Repetition
1	EN AW 6060	460	1	2
2			4	2
3			8	2
4		480	1	2
5			4	2
6			8	2
7	EN AW 6082	460	1	2
8			4	2
9			8	2
10		480	1	2
11			4	2
12			8	2

Extrusion forces were recorded during the trials (Fig. 2). The differences in force levels at different ram speeds are clearly distinguishable at the beginning of the extrusion processes. However, at higher ram speed, extrusion force decreases faster and thus the difference becomes less and less distinguishable as the extrusion process proceeds. The reasons behind the fast decrease in force level at higher ram speed are more heat generation, less heat loss and thus, more steeply decreased flow stress.

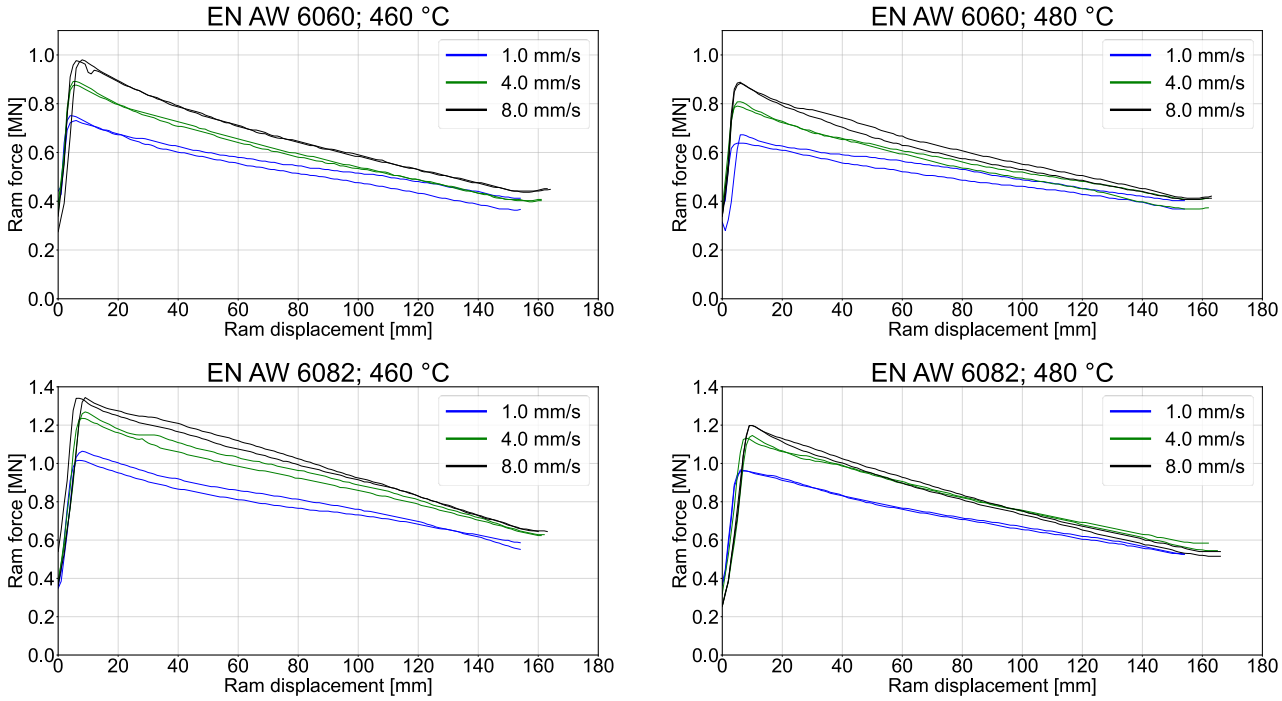

Fig. 2: Extrusion force obtained from the press.

Temperature histories of the flowing material near the die exit were also recorded with a thermocouple. The thermocouple was installed into the die through a hole and the temperature was measured approximately 1 mm under the die surface at the die land. However, due to some technical failure, temperature recording was not successful for certain experiments (Fig. 3).

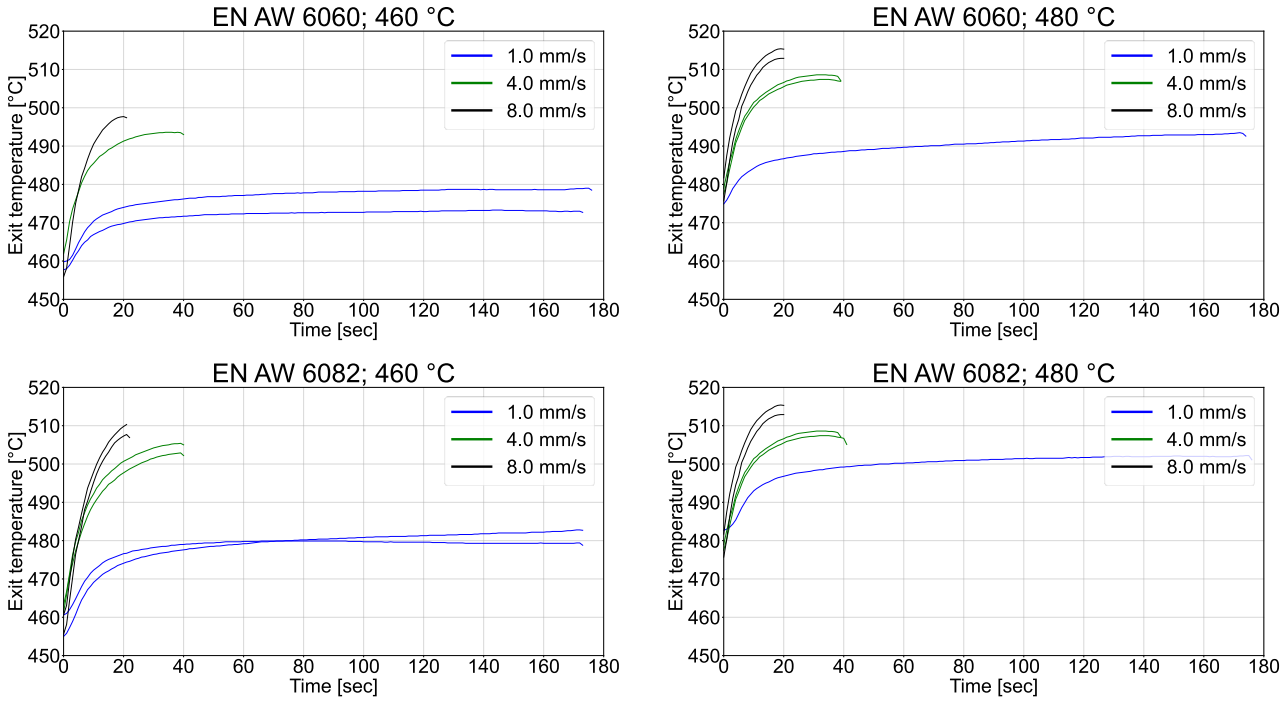

Fig. 3: Material temperature measured near the die land.

Material Characterization

During a hot extrusion process, the material undergoes large plastic deformation at high temperatures and strain rates. Hence, for an accurate simulation of a hot extrusion process, flow stress data for an appropriate range of temperatures and strain rates are necessary. In this work, flow stresses were obtained from hot compression tests conducted in a high-speed deformation dilatometer “Bähr

DIL805A/D". Cylindrical specimens with 5 mm diameter and 10 mm height (Fig. 4) were compressed at three temperatures (450 °C, 500 °C, 550 °C) and three strain rates (0.1 s^{-1}, 1 s^{-1}, 10 s^{-1}) for each temperature. Each test was repeated three times to ensure the validity.

Fig. 4: Cylindrical specimens after compression test.

During a compression test at a strain rate of 10 s^{-1}, temperature rises almost by 10 °C. Hence, temperature compensated flow stress data were computed by linear interpolation. Each flow stress curve obtained from compression tests was extrapolated by Voce hardening law:

$$k_f(\varphi) = \sigma_\infty - \left(\sigma_\infty - k_{f0}\right) * e^{-m\varphi}. \quad (1)$$

whereas k_{f0} is the initial yield stress, σ_∞ and m are the hardening parameters. It was also observed in the preliminary simulations that the strain rate reaches almost up to 200 s^{-1} for extrusion process at 8 mm/s ram speed. Hence, flow stress data were extrapolated at a strain rate of 100 s^{-1} and 200 s^{-1} according to [17].

$$k_f = k_{f1} * \left(\frac{\dot{\varphi}}{\dot{\varphi}_1}\right)^m. \quad (2)$$

whereas k_{f1} and k_f are the stresses at strain rates of $\dot{\varphi}_1$ and $\dot{\varphi}$ respectively, and

$$m = \frac{d\ log\ k_f}{d\ log\ \dot{\varphi}}. \quad (3)$$

Flow Stress Look Up Table in HyperXtrude was chosen as the constitutive model which allows direct input of the flow stress data (Fig. 5 & Fig. 6) at various strains, strain rates and temperatures in the form of a 3D table. Hence, no parameter identification is necessary. Flow stress at a particular strain, strain rate and temperature is obtained by using trilinear interpolation.

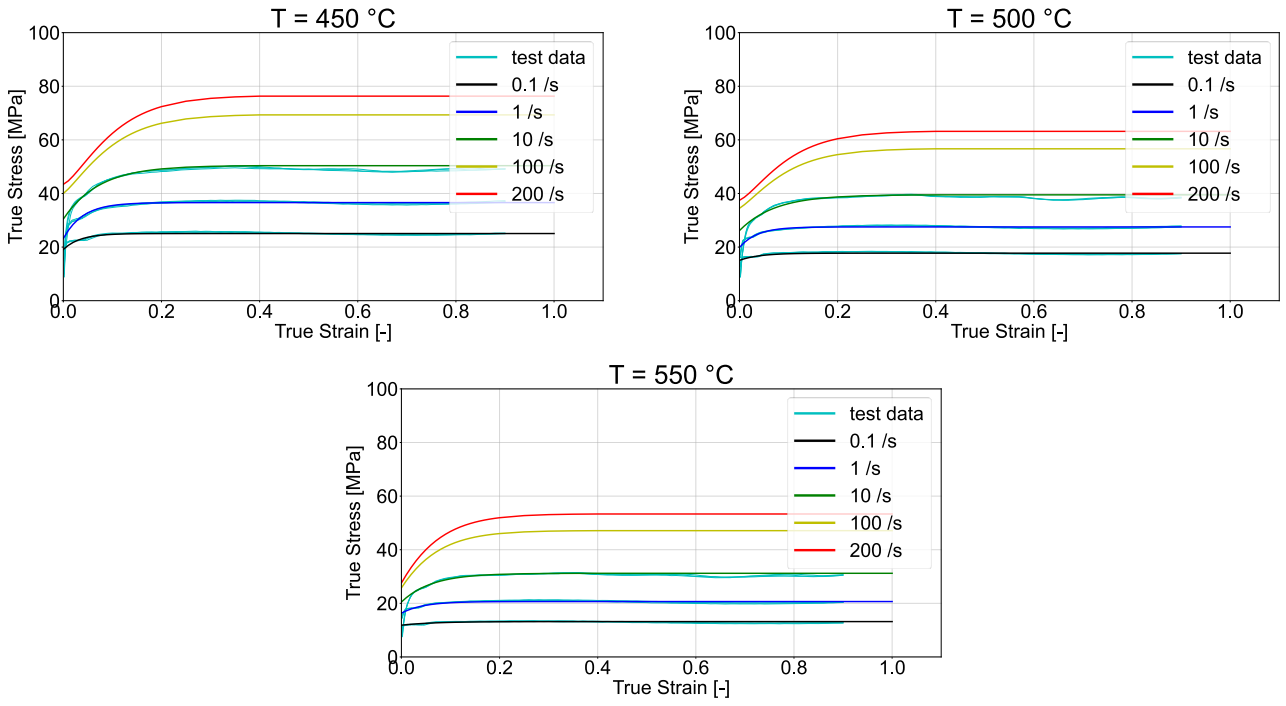

Fig. 5: Flow stress data for EN AW 6060.

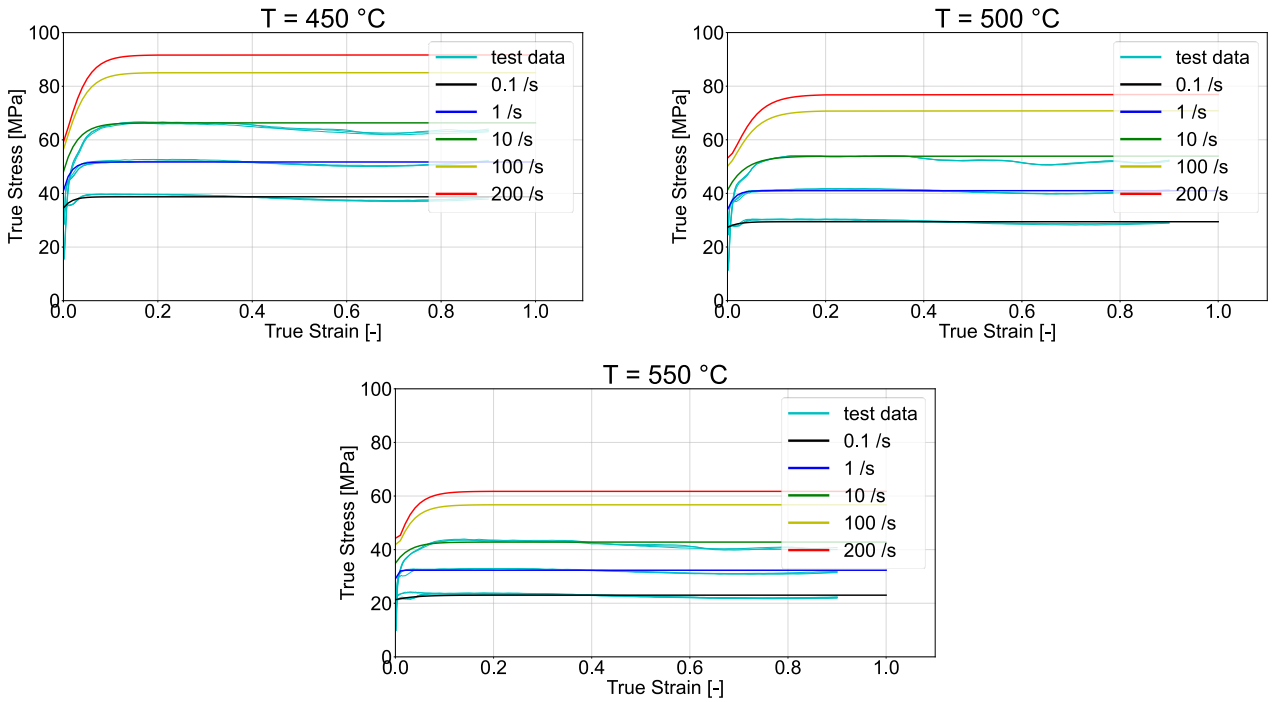

Fig. 6: Flow stress data for EN AW 6082.

Modeling and Simulation

Mesh. Only 1/4th of the total geometry was modeled using symmetric boundary conditions (Fig. 7, left). The model consists of four parts: billet, pocket, bearing, and profile (Fig. 7, right). Billet and pocket were meshed with 3D 4-node tetrahedral elements, while bearing and profile were meshed with 3D 6-node prismatic elements. A mesh convergence study was carried out to ensure the mesh insensitivity of the model. Three different mesh sizes were investigated (Table 2). The results were found to be similar in terms of extrusion force. Based on this study, the model with the coarse mesh was chosen for subsequent simulations.

Table 2: Mesh convergence study.

Mesh	No. of elements	No. of nodes	Computation time (normalized)
Coarse	171941	36018	0.26
Medium	232567	48024	0.63
Fine	331010	67075	1.0

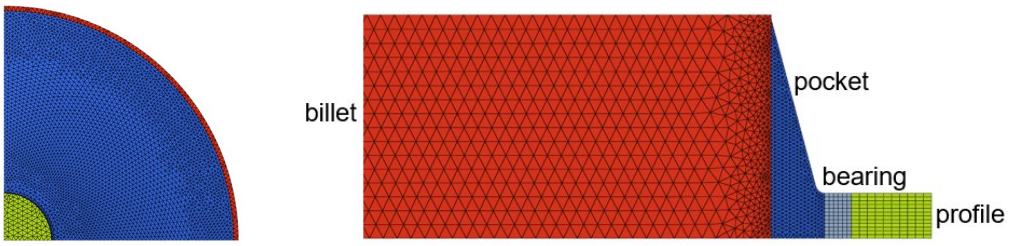

Fig. 7: Front view (left) and side view (right) of the symmetric FE-model.

Boundary Condition. Symmetric boundary conditions were applied *(SymmetryBC)* to the planes of symmetry and thus only 1/4th of the whole geometry was modeled. The heat exchange at the tool-billet interface was defined by a thermal boundary condition with convective heat coefficient of 3000 W/m^2*°C (default in HyperXtrude). Initially, Extrusion trial for EN AW 6060 at 460 °C and 1 mm/s ram speed (Trial-1 in Table 1) was simulated using different friction models (Table 2) with a goal to calibrate the friction coefficient where applicable.

Table 2: Initial simulations with different combinations of friction models.

	Simulation-1	Simulation-2	Simulation-3	Simulation-4	Simulation-5
Solid Wall	Slip	SlipVelocity (1.0E+09)	Coulomb (0.02)	ViscoPlastic (0.3)	Stick
Bearing	ViscoPlastic (0.3)	ViscoPlastic (0.3)	ViscoPlastic (0.3)	ViscoPlastic (0.3)	ViscoPlastic (0.3)

The friction coefficient for SlipVelocity was taken from [18], Coulomb according to [15], and ViscoPlastic according to [18]. All the friction models except the Stick BC significantly underestimated the extrusion force and showed convergence issue. Hence, in the next step, Stick BC was applied to the SolidWall regions (e.g., around the billet surface and pocket-die interface) and the friction coefficient for ViscoPlastic BC in the bearing region was varied from default 0.3 up to maximum value 1.0 (full stick). The best agreement between experiment and simulation was achieved for full stick condition at the bearing region. Finally, all the extrusion trials were simulated with full stick friction in SolidWall as well as bearing region.

Results and Discussion

Using full stick condition, for both alloys at 1 mm/s ram speed, experiment and simulation agree very well in terms of extrusion force (Fig. 8) as well as exit temperature (Fig. 9). This indicates that the calibrated friction condition is transferable within a temperature range of at least 20 °C.

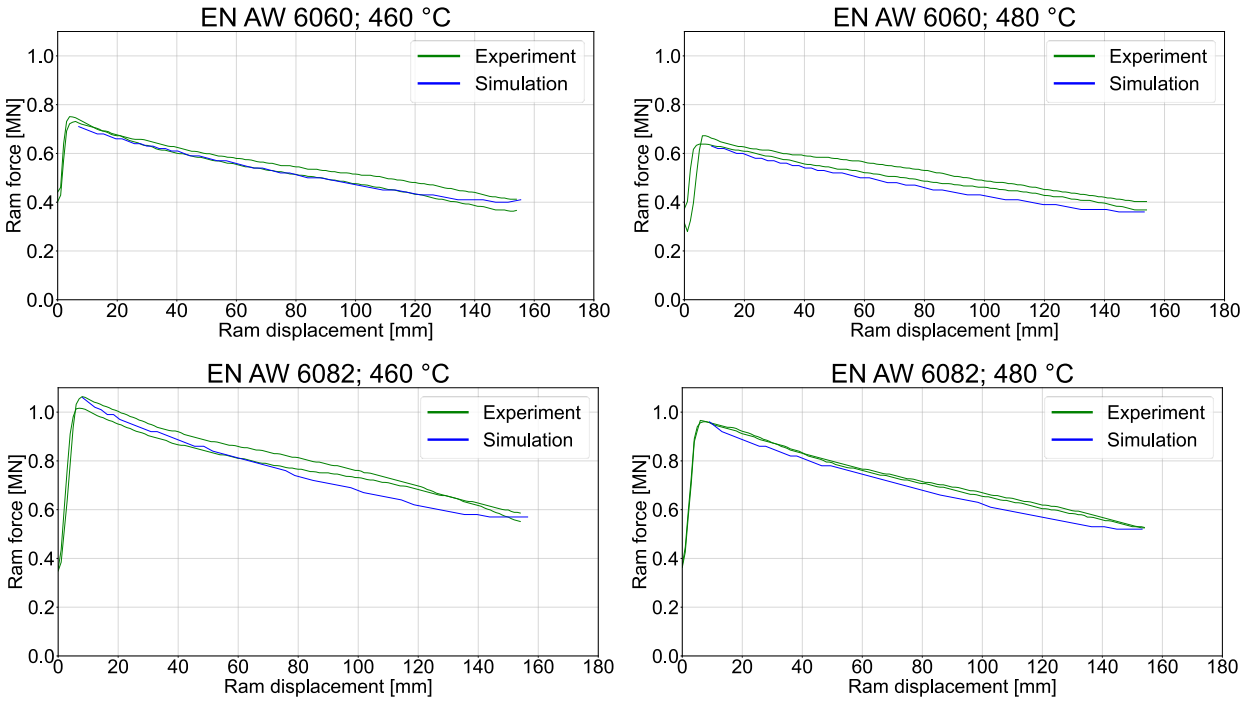

Fig. 8: Experiment vs. simulation in terms of extrusion force (1 mm/s ram speed).

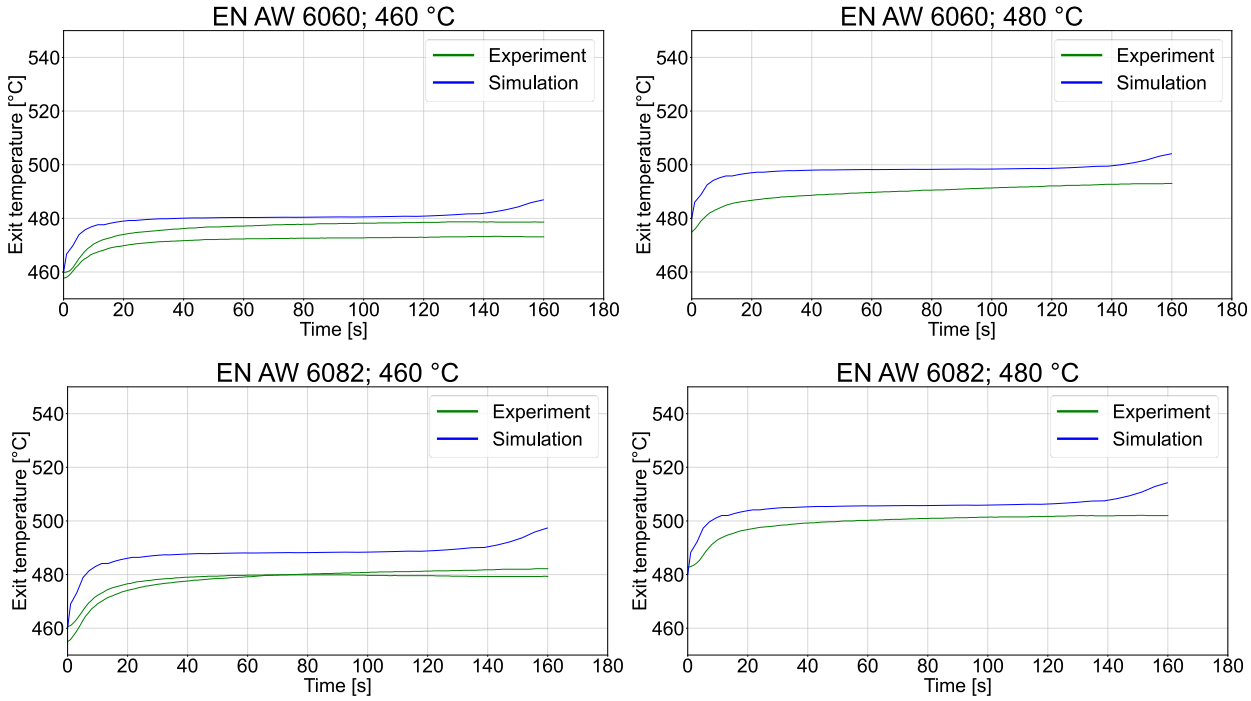

Fig. 9: Experiment vs. simulation in terms of material temperature near die land (1 mm/s ram speed).

Rest of the trials (ram speed 4 mm/s and 8 mm/s) show reasonably good agreement in terms of friction force (Fig. 10 & Fig. 11); however, there is a small deviation (<10%), especially for EN AW 6060, which indicates that there might be a mild influence of the ram speed on friction parameter. The deviation might also come from the extrapolated flow curves at high strain rates which needs to be further investigated.

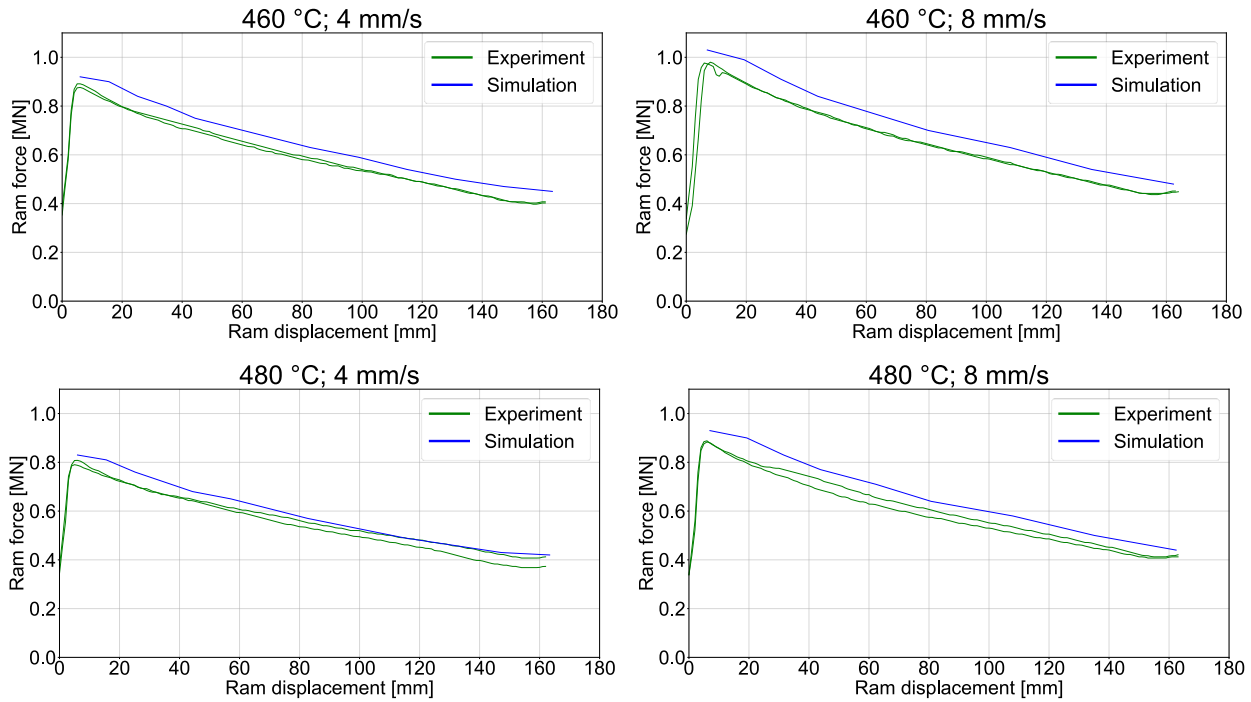

Fig. 10: Experiment vs. simulation in terms of extrusion force for EN AW 6060.

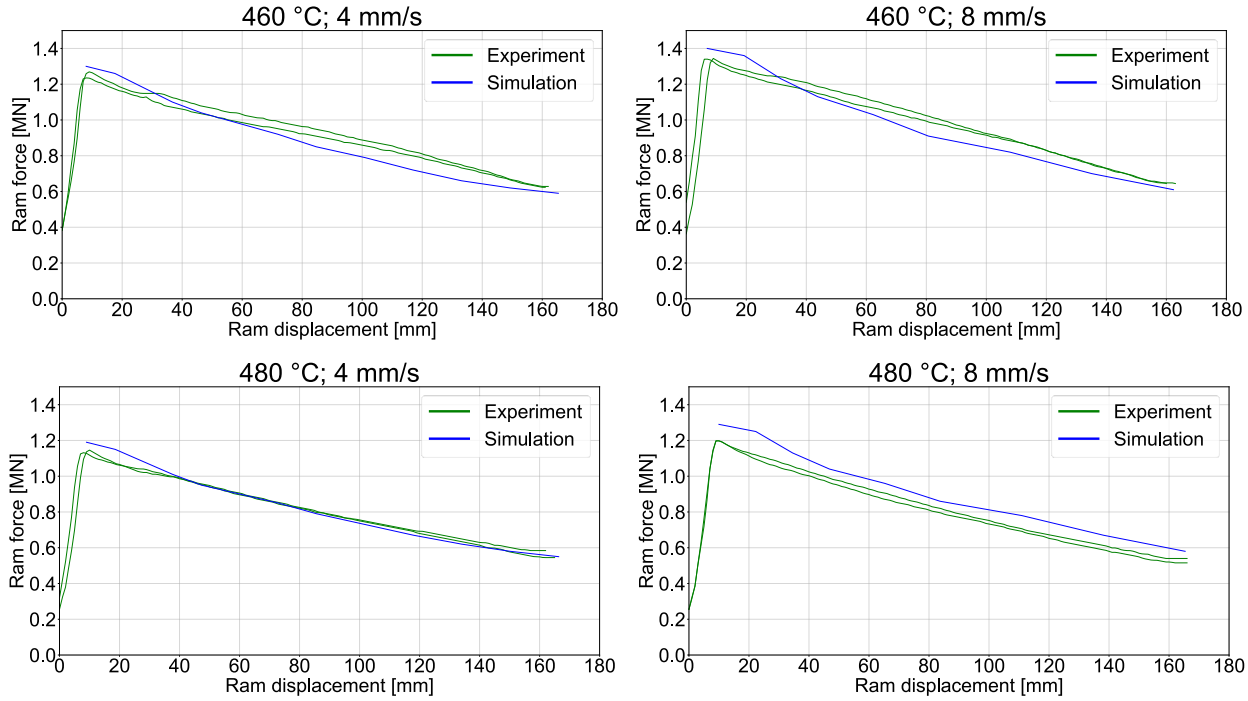

Fig. 11: Experiment vs. simulation in terms of extrusion force for EN AW 6082.

The exit temperature in simulation deviates almost up to 40 °C for extrusion trials with higher ram speed (Fig. 12 & Fig. 13). This indicates that the default thermal properties of the materials as well as default thermal boundary conditions might not be accurate enough.

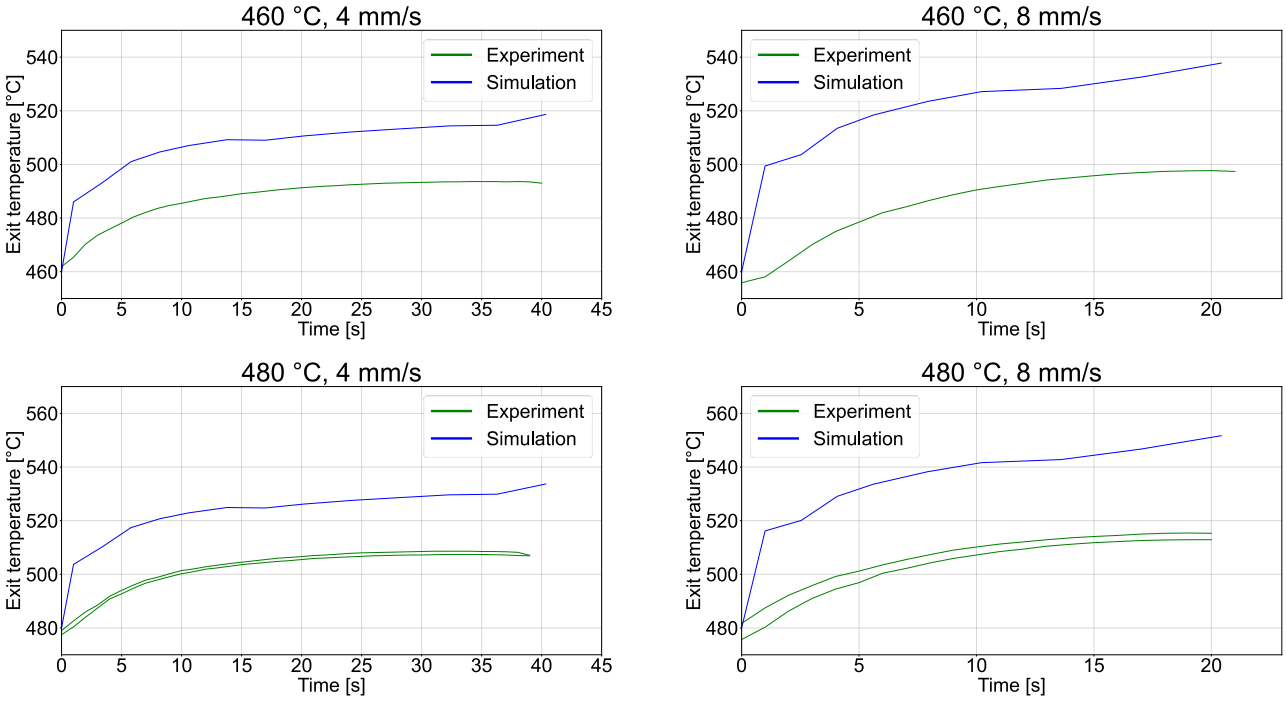

Fig. 12: Experiment vs. simulation in terms of material temperature near die land for EN AW 6060.

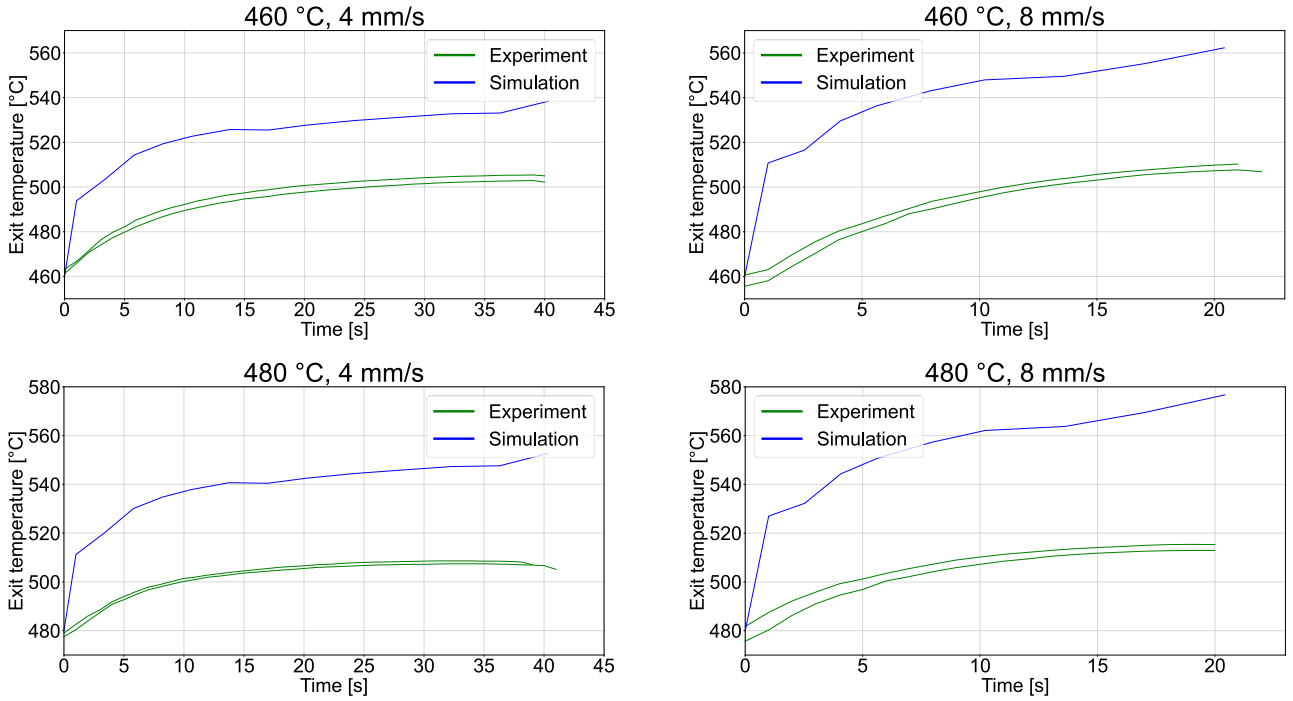

Fig. 13: Experiment vs. simulation in terms of material temperature near die land for EN AW 6082.

Summary

Based on the experimental investigations as well as simulation results, the following conclusions can be drawn:

- Sticking friction in the SolidWall regions is appropriate which complies with several other research papers [10-14].
- Fully stick friction (ViscoPlastic, coefficient = 1.0) in the Bearing region is appropriate for slow extrusion (ram speed of 1 mm/s in our case). It might slightly overpredict the extrusion force for higher ram speed (4 mm/s and 8 mm/s in our case). However, the prediction in simulation is still reasonably good.
- Default thermal properties of the materials and thermal boundary conditions need to be investigated in detail for an accurate prediction of the material temperature.

References

[1] P. Hora, C. Karadogan, L. Tong, Numerische Modellierung thermischer und tribologischer Randbedingungen, in: Conference Proceedings Extrusion Zurich (2005).

[2] C. Karadogan, F. Vanini, L. Tong, P. Hora, State of the Art and Potential Development of Digital Extrusion Modeling, in: Light Metal Age 63 (2005), 40-43.

[3] H. S. Valberg, Applied Metal Forming including FEM Analysis, first edition, Cambridge University Press, Cambridge, 2010.

[4] T. Wanheim, N. Bay, A model for friction in metal forming processes, in: Ann. CIRP 27 (1976) 189–193.

[5] P. Hora, C. Becker, L. Tong, J. Maier, S. Müller, Advanced frictional models for extrusion application, in: Key Engineering Materials 585 (2013) 41-48.

[6] L. Tong, FE Simulation of Bulk Forming Processes with a Mixed Eulerian-Lagrangian Formulation, PhD Thesis, ETH-Zurich (1995).

[7] C. Karadogan, Advanced methods in numerical modeling of extrusion processes, PhD Thesis, ETH-Zurich (2005).

[8] L. Wang, Modelling of friction for high temperature extrusion of aluminium alloys, PhD Thesis, TU Delft (2012).

[9] D. Horwatitsch, Entwicklung eines Reibmodells für hohe Temperaturen und hohe Umformgrade (Development of a Friction Model for High Temperatures and High Strains), In: Steinhoff, K. (ed.): Berichte zur Metallformgebung – vol 3. Kassel: Kassel university press, 2013.

[10] M. G. L. Crosio, Virtual analysis of welds formation during direct extrusion processes, PhD Thesis, ETH-Zurich (2020).

[11] C. Bertoli, Optimization of Hybrid Extrusion Dies with Internal Cooling Channels, PhD Thesis, ETH-Zurich (2020).

[12] M. Negozio, R. Pelaccia, L. Donati, B. Reggiani, L. Tomesani, T. Pinter, FEM Validation of Front End and Back End Defects Evolution in AA6063 and AA6082 aluminum alloys profiles, in: Procedia Manufacturing 47 (2020) 202–208.

[13] B. Reggiani, A. Segatori, L. Donati, L. Tomesani, Prediction of charge welds in hollow profiles extrusion by FEM simulations and experimental validation, in: The International Journal of Advanced Manufacturing Technology 69 (2013) 5-8.

[14] T. Sheppard, EXTRUSION OF ALUMINIUM ALLOYS, first edition, Springer Science + Business Media, Dordrecht (1999).

[15] L. Donati, L. Tomesani, M. Schikorra, N. Ben Khalifa, A.E. Tekkaya, Friction model selection in FEM simulations of aluminium extrusion, in: Int. J. Surface Science and Engineering 4 (2010) 27-41.

[16] W. Z. Misiolek, R. M. Kelly, Extrusion of aluminium alloys, ASM Handbook, 2005, pp. 522-527.

[17] E. Doege, H. M. Nolkemper, I. Saeed, Fließkurvenatlas metallischer Werkstoffe, Hanser Verlag München Wien (1986).

[18] Altair HyperXtrude Manual.